CrossMark
[Click for updates](#)

Atmosphere-Ocean
Publication details, including instructions for authors and subscription information:
http://www.tandfonline.com/loi/tato20

Atmospheric and Terrestrial Water Balances of Labrador's Churchill River Basin, as Simulated by the North American Regional Climate Change Assessment Program

Jonas Roberts[a] & Ken Snelgrove[a]
[a] Faculty of Engineering and Applied Science, Memorial University of Newfoundland, St. John's, Newfoundland and Labrador, Canada
Published online: 16 Apr 2015.

Atmospheric and Terrestrial Water Balances of Labrador's Churchill River Basin, as Simulated by the North American Regional Climate Change Assessment Program

Jonas Roberts* and Ken Snelgrove

Faculty of Engineering and Applied Science, Memorial University of Newfoundland, St. John's, Newfoundland and Labrador, Canada

[Original manuscript received 14 October 2014; accepted 18 February 2015]

ABSTRACT *In an effort to understand the sources of uncertainty and the physical consistency of climate models from the North American Regional Climate Change Assessment Program (NARCCAP), an ensemble of general circulation models (GCMs) and regional climate models (RCMs) was used to explore climatological water balances for the Churchill River basin in Labrador, Canada. This study quantifies mean atmospheric and terrestrial water balance residuals, as well as their annual cycles. Mean annual atmospheric water balances had consistently higher residuals than the terrestrial water balances due, in part, to the influences of sampling of instantaneous variables and the interpolation of atmospheric data to published pressure levels. Atmospheric and terrestrial water balance residuals for each ensemble member were found to be consistent between base and future periods, implying that they are systemic and not climate dependent. With regard to the annual cycle, no pattern was found across time periods or ensemble members to indicate whether the monthly terrestrial or atmospheric root mean square residual was highest. Because of the interdependence of hydrological cycle components, the complexity of climate models and the variety of methods and processes used by different ensemble members, it was impossible to isolate all causes of the water balance residuals. That being said, the residuals created by interpolating a model's native vertical resolution onto NARCCAP's published pressure levels and the subsequent vertical interpolation were quantified and several other sources were explored. In general, residuals were found to be predominantly functions of the RCM choice (as opposed to the GCM choice) and their respective modelling processes, parameterization schemes, and post-processing.*

RÉSUMÉ *[Traduit par la rédaction] Afin de mieux comprendre les sources d'incertitude et la cohérence physique dans les modèles climatiques du* North American Regional Climate Change Assessment Program *(NARCCAP), nous avons utilisé un ensemble de modèles de circulation générale et de modèles climatiques régionaux pour explorer les bilans hydrologiques climatologiques pour le bassin du fleuve Churchill, au Labrador, au Canada. Cette étude quantifie les résidus moyens des bilans hydrologiques terrestres et atmosphériques de même que leurs cycles annuels. Les bilans hydrologiques atmosphériques annuels moyens ont constamment eu des résidus plus élevés que les bilans hydrologiques terrestres, notamment à cause des effets de l'échantillonnage de variables instantanées et de l'interpolation de données atmosphériques en fonction des niveaux de pression publiés. Les résidus des bilans hydrologiques atmosphériques et terrestres pour chaque membre de l'ensemble se sont révélés cohérents entre les périodes de base et future, ce qui implique qu'ils sont systémiques et non liés au climat. En ce qui concerne le cycle annuel, nous n'avons pas trouvé de configuration entre les périodes ou les membres de l'ensemble qui indiquerait si le résidu quadratique moyen terrestre ou atmosphérique est plus élevé. Étant donné l'interdépendance des éléments du cycle hydrologique, la complexité des modèles climatiques et la variété des méthodes et des processus utilisés par les différents membres de l'ensemble, il a été impossible d'isoler toutes les causes des résidus des bilans hydrologiques. Cela dit, nous avons quantifié les résidus créés par l'interpolation de la résolution verticale native d'un modèle en fonction des niveaux de pression publiés par le NARCCAP et par l'interpolation verticale subséquente et nous avons exploré plusieurs autres sources. De manière générale, il ressort que les résidus sont surtout fonction du choix des modèles climatiques régionaux (par opposition au choix des modèles de circulation générale) ainsi que de leurs processus de modélisation, de leurs schémas de paramétrisation et de leur post-traitement.*

KEYWORDS water balance; water balance residual; general circulation models; regional climate models; ensemble analysis; model error

*Corresponding author's email: jonaspmr@gmail.com

1 Introduction

There is a growing realization in scientific and engineering communities that a changing global climate requires the use of high-resolution climate models to aid in the design and planning of large-scale water resource projects (Dimri, 2012). Simple use of historical climate records is inadequate when planning for mean hydrological states and extreme events because both are influenced by climate change (Trenberth, Dai, Rasmussen, & Parsons, 2003). In order to determine the effectiveness of a climate model's ability to simulate the hydrological cycle, and therefore its usefulness to water resource managers, its atmospheric and terrestrial water balances must be examined (Berbery & Rasmusson, 1999). It is recognized that simulation of the water cycle and the wide variety of physical processes involved is a key factor in a model's ability to effectively simulate current and future climates (Chahine, 1992; Hack, Kiehl, & Hurrell, 1998). Hu, Oglesby, and Marshall (2005) stated that the "examination of moisture simulation as it relates to climate likely holds the key to our understanding and eventually resolving issues surrounding model uncertainty."

Both general circulation models (GCMs) and high-resolution regional climate models (RCMs) play important roles in developing an accurate water balance (Berbery & Rasmusson, 1999). Moisture is involved in a diverse range of temporal and spatial scales: from minutes to decades and from the micro-physical level up to global circulation. It has been found that water climatologies are different from model to model for a number of reasons (Wang & Paegle, 1996), some of which will be explored in this work. Additionally, differences in climate sensitivity (defined as the equilibrium global mean temperature increase caused by doubling atmospheric CO_2 concentrations) among climate models can be explained in part by differences in projected moisture levels, for which the simulation and parameterization of surface and boundary layer processes are largely responsible (Hu et al., 2005). It is apparent that moisture and its motion are major climatological factors for any basin (Liu & Stewart, 2003).

a *Motivation*

There are several reasons for undertaking a water balance study. This section discusses a selection of motivations for, and examples of, existing studies.

One motivation is to examine model uncertainty, improve climate model processes and parameterization, and validate the physical consistency of climate models. In this vein, Music and Caya (2007) performed a comprehensive validation of water budget components of a basin with respect to the annual mean and annual cycle. Roads, Chen, Kanamitsu, and Juang (1998) evaluated climate models by examining the vertical distribution of water budget residuals as well as the fit of primary variables to observations. These types of studies typically focus on one or two specific climate models.

Another common motivation is to understand the hydrologic processes of a region and how they evolve over time. Strong et al. (2002), as part of the Global Energy and Water Exchanges (GEWEX) project, performed a water budget analysis on the Mackenzie River basin. The primary objective of GEWEX was to quantify all aspects of the hydrological cycle of the Mackenzie River basin for purposes of investigating the impacts of climate change on the water budget. Jin and Zangvil (2010) found that moisture convergence and precipitable water tendency balance precipitation and evaporation over the eastern Mediterranean and are strongly correlated in time.

A third motivation for water balance studies is to obtain approximations for difficult-to-observe variables. Serreze et al. (2002) use National Centers for Environmental Prediction/National Center for Atmospheric Research (NCEP/NCAR) global reanalysis data to calculate precipitation minus evapotranspiration (*P*–*E*) from the moisture flux convergence for several large Arctic basins. Seneviratne, Viterbo, Lüthi, and Schär (2004) and Hirschi, Seneviratne, and Schär (2006) showed that one can effectively estimate basin-scale terrestrial water storage using atmospheric and terrestrial water balance equations, plus streamflow measurements.

Accordingly, the purpose of this paper is twofold: (i) to investigate the physical consistency of a selection of RCMs forced by various GCMs over the Churchill River basin in Labrador, Canada, and (ii) to identify reasons why the atmospheric and terrestrial water budgets do not balance.

b *Study Region*

The Churchill River, located in Labrador, Canada, is 856 km long and drains roughly 92,500 km^2. The basin is the site of the existing Churchill Falls hydroelectric facility and the proposed Lower Churchill Hydroelectric Project. Figure 1 presents a map of the basin and includes major water features and population centres. A map showing the topography and common grid resolution (0.25 degrees) to which all the models in this study were re-gridded can be found in Roberts and Snelgrove (2015).

The basin is typically snow covered for more than half the year because snowfall is the most common precipitation type from October to May. According to Environment Canada's in-situ meteorological stations, mean annual precipitation ranges from 850 to 950 mm, with a relatively even split between rain and snow. The mean annual temperature ranges from −5° to 0°C, with record winter extremes below −40°C and record summer extremes surpassing 30°C (Environment Canada, 2014).

Because of the large amount of snow accumulation in winter, spring melt is a predominant feature in the annual hydrograph of the Churchill River. However, the spring melt signal is subdued by the existence of the Churchill Falls hydroelectric facility and its associated reservoirs and control structures. Roughly three-quarters of the runoff from the Churchill River originates upstream of Churchill Falls.

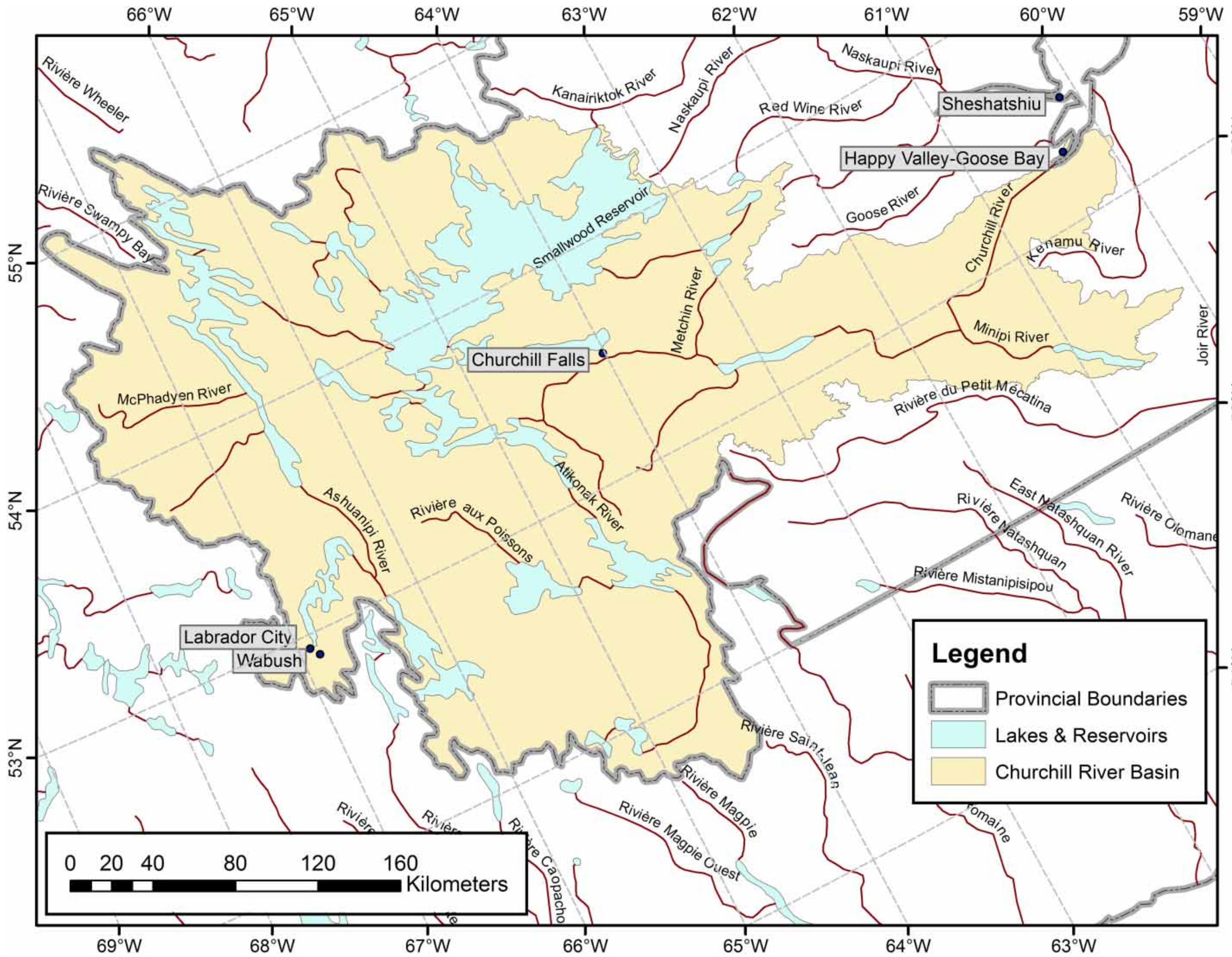

Fig. 1 Churchill River basin.

Two types of soil are predominant in the basin: well-drained and acidic podzolic soil and organic soil with poor drainage. In addition to the extensive wetlands, coniferous black spruce forest is ubiquitous, though in some areas a variety of hardwood species can be found. The dominant features in the northwestern portion of the basin are the reservoirs for Churchill Falls. Downstream of Churchill Falls, the eastern half of the basin is at elevations below 400 m and has a well-defined drainage pattern with steep tributary slopes and relatively few wetlands. Glacial activity resulted in rugged topography throughout the basin, with high points in the western headlands reaching 1550 m, down to near sea level in the east (Nalcor Energy, 2009).

Early work on water balances was limited to basins larger than 2×10^6 km^2, due primarily to low radiosonde observation density and sampling frequency (Min & Schubert, 1997; Rasmusson, 1968). More recently, a commonly touted critical size for water balance computations using atmospheric reanalysis is on the order of 10^5 km^2. That being said, Hirschi et al. (2006) performed water balances on three basins similar in size to the Churchill River basin (84,144, 85,223, and 94,836 km^2) with acceptable imbalances. All studies mentioning critical basin size have used observations, analyses, and reanalysis datasets with roughly 1 degree resolution and larger. Higher resolution climate models, such as those used in this study (50 km horizontal grid spacing, resulting in the basin being represented by 37 grid points, and 3-hour sampling frequency) should be able to provide reliable water balances for domains the size of the Churchill River basin (Jin & Zangvil, 2010). The 0.25 degree grid to which all model output was re-gridded does not provide additional information in this respect, though it does allow for more consistent representation of the irregular basin boundaries.

c *Literature Review*

There is a great deal of interdependence within modelling processes, as well as components of the water cycle, making the isolation of a single source of imbalance difficult. Every factor and process involved in water cycle simulation is potentially important and should not be discounted without just cause. The following review highlights potential causes of water balance residuals from published literature. These potential causes are organized into categories below.

1 VERTICAL COORDINATE SYSTEM AND SPATIAL RESOLUTION

The conversion from a model's native vertical coordinate system to published pressure levels has been known to introduce mass imbalances up to a relative magnitude of 100% depending on the region and variable of interest (Berbery & Rasmusson, 1999; Serreze et al., 2002; Trenberth, 1991). These imbalances are mostly systemic and decrease in magnitude as vertical resolution increases. Similarly, some vertical coordinate systems are more susceptible to the introduction of errors during vertical integration than others (e.g., pressure levels versus sigma levels (Liu & Stewart, 2003)).

Complex topography leads to difficulties in simulating water vapour transport at lower levels, though a sigma level approach has been shown to resolve the atmospheric boundary layer better and reduce this aspect of bias (Chen, Norris, & Roads, 1996; Liu & Stewart, 2003). This is not a predominant factor in the current study because the topography of the basin is relatively uncomplicated compared with mountainous regions in other studies. Errors in surface pressure fields and topography, in addition to the vertical resolution and post-processing, also play a role in the balancing of the water budget (Min & Schubert, 1997).

Roads et al. (1998) found that initializing an 18-level climate model with a 28-level analysis simulation produced larger budget imbalances than when vertical levels aligned (despite the application of a variety of digital filters), showing that discrepancies between GCM and RCM vertical levels are contributing factors.

Liu and Stewart (2003) postulated that a small domain size and low spatial resolution (e.g., 15 grid points at 2.5 degree resolution) would not effectively capture local convection events, drastically affecting local water content.

2 TEMPORAL RESOLUTION AND SAMPLING FREQUENCY

Inadequate sampling of instantaneous variables (e.g., wind) cannot be compensated for by using long sampling periods, and it has been found that moisture convergence is the variable most strongly affected by sampling frequency (Chen et al., 1996). Imbalances as large as the moisture convergence itself over mid-latitude storm tracks were found when using 12-hourly, or even sometimes 6-hourly, sampling. Roads et al. (1998) discussed this sampling issue while investigating non-linear fluxes.

As a subset of moisture convergence, the inability to resolve low-level jets also leads to errors, though in North America this issue is concentrated primarily in the Great Plains regions (Chen et al., 1996). Resolution of the diurnal cycle is important to regions with low-level jets (Berbery & Rasmusson, 1999), which are not major sources of influence over the Churchill River basin. They recommend eight timesteps per day (3-hour intervals) to effectively capture the diurnal cycle, especially for smaller basins.

3 MODEL PROCESSES AND PARAMETERIZATION

Parameterizations of smaller scale turbulent processes, such as condensation, boundary layer moisture flux, boundary layer temperature flux, and net radiation flux (shortwave and longwave) at the surface all contribute to the water budget. Jin and Zangvil (2010) argue that the residuals in atmospheric water balances can be attributed mainly to the theoretical treatment of the water budget equations. They found that assimilating empirical data decreased residuals, though this approach is only viable when using reanalysis models, such as NCEP or the European Centre for Medium-Range Weather Forecasts (ECMWF) 40-year Reanalysis (ERA-40).

Ruane (2010) found that regions where seasonal precipitation draws primarily from atmospheric moisture convergence are sensitive to dynamical processes (e.g., large-scale waves, circulations, or conditions favourable to mesoscale activity), whereas regions with a high recycling ratio are more sensitive to processes affecting atmospheric stability (e.g., land-surface interaction, boundary layer physics, and convective processes).

Global fields of precipitation, temperature, and motion strongly depend on land-surface evapotranspiration (Shukla & Mintz, 1982), which is generally parameterized as the sum of soil evaporation, vegetation evaporation, and vegetation transpiration (Wang & Dickinson, 2012). Different land-surface models give a wide range of ratios of transpiration to total evapotranspiration. Parameterized latent heat (as evapotranspiration) typically uses about 60% of net surface radiation, though it can vary between models from below 50% to almost 90% (Trenberth, Fasullo, & Kiehl, 2009; Wang & Dickinson, 2012), contributing to inter-model discrepancies.

Terrestrial water storage is a key part of the water balance and hydrological cycle because it determines the partitioning of the water and energy fluxes at the land surface (Mueller, Hirschi, & Seneviratne, 2011). Although the importance of the effect of soil moisture on terrestrial water balances is intuitive, it is also important for atmospheric water balances in regions with high precipitation recycling. As with the evapotranspiration ratio above, estimates of soil moisture on a regional scale differ greatly from model to model (Hirschi et al., 2006; Reichle, Koster, Dong, & Berg, 2004; Schär, Lüthi, Beyerle, & Heise, 1999).

d *Climate Models*

The North American Regional Climate Change Assessment Program (NARCCAP; http://www.narccap.ucar.edu/about/index.html) is an international collaboration whose primary purpose is to create high-resolution climate simulations of North America in order to examine uncertainties within the member RCMs and the driving GCMs (Mearns et al., 2009). The NARCCAP ensemble members simulate a base period (1971–2000) and a future period (2041–2070) under the Intergovernmental Panel on Climate Change (IPCC) A2 emission scenarios (IPCC, 2000) using various map projections at

TABLE 1. NARCCAP RCM characteristics.

RCM	Reference	Dynamics Core	Vertical Levels	Vertical Coord-inates	Convective Parameter-ization	Land-Surface Scheme	# Veg. Classes	Buffer Zone Size[a]
CRCM	Caya and Laprise (1999)	Nonhydrostatic, compressible	29	Gal-Chen scaled-height	Mass-flux	CLASS	21	10
HRM3	Jones et al. (2004)	Hydrostatic, compressible	19	Hybrid terrain following -pressure	Mass-flux (incl. downdraft)	MOSES	53	8
MM5I	Grell, Dudhia, and Stauffer (1993)	Nonhydrostatic, compressible	23	Sigma	Kain-Fritsch2 mass-flux	NOAH	16	15
RCM3	Giorgi, Marinucci, and Bates (1993a), Giorgi, Marinucci, Bates, and De Canio (1993b), Pal, Small, and Eltahir (2000), Pal et al. (2007)	Hydrostatic, compressible	18	Terrain following	Grell (with Fritsch-Chappell closure)	BATS	19	13
WRFG	Skamarock et al. (2005)	Nonhydrostatic, compressible	35	Terrain following	Grell	NOAH	24	10.5

[a]Number of RCM grid points at each lateral forcing boundary.

TABLE 2. NARCCAP GCM characteristics.

GCM	Reference	Horizontal Atmospheric Resolution (latitude × longitude)	Vertical Layers	Top Level	Climate Sensitivity
CCSM	Collins et al. (2006)	$1.4° \times 1.4°$	26	2.2 hPa	2.7°C
CGCM3	Flato (2005), Scinocca and McFarlane (2004)	$1.9° \times 1.9°$	31	1 hPa	3.4°C
GFDL	GFDL (2004)	$2.0° \times 2.5°$	24	3 hPa	3.4°C
HADCM3	Gordon et al. (2000), Pope, Gallani, Rowntree, and Stratton (2000)	$2.5° \times 3.75°$	19	5 hPa	3.3°C

50 km resolution. To give an idea of the variety of modelling and parameterization strategies employed by different modelling groups, a brief synopsis of the RCMs and GCMs used in this study are presented in Tables 1 and 2 respectively.

2 Methodology

To determine the movement of moisture into and out of a basin, the atmospheric and terrestrial water balances were calculated for mean monthly climatologies. The equations for each water balance are presented below (Eqs (1) and (2); see Rasmusson (1968) and Peixoto and Oort (1992) for more details). The units of each component in Eqs (1) and (2) were converted to cubic metres per second for consistency across each water balance. For the Churchill River basin 1070.6 $m^3\ s^{-1}$ is approximately 1.00 mm d^{-1}.

$$-\frac{\partial W}{\partial t} - \nabla_H \vec{Q} = P - E + \varepsilon_A, \qquad (1)$$

$$R + \frac{\partial s}{\partial t} = P - E + \varepsilon_T, \qquad (2)$$

where

W is the precipitable water content of the atmosphere;
$-\nabla_H \vec{Q}$ is the atmospheric moisture convergence;
$\vec{Q}$ is the vertically integrated horizontal water vapour flux;
$P - E$ is precipitation minus evaporation;
R is the land-surface runoff;
s is terrestrial water storage, including snow pack and soil moisture;
ε_A is the atmospheric water balance residual;
ε_T is the terrestrial water balance residual; and
t is time.

The atmospheric moisture convergence, which reflects how much water is advected into or out of a basin via the atmosphere over a period of time, is a large component of atmospheric water balances, and a detailed description of its computation can be found in Seneviratne et al. (2004). The horizontal water vapour flux was calculated for each grid point by multiplying the specific humidity by the meridional and zonal (south to north and west to east, respectively) wind components, to obtain two respective values of flux for each grid point. The vertical integration of the horizontal water vapour flux was then performed in the Grid Analysis and Display System (GrADS), using the function vint(), which takes the sum of the mass-weighted layers between the surface (as defined by surface pressure) and the top of the atmosphere (as defined by the uppermost pressure level available, 50 hPa). This provided the total vertical column amount of moisture flux in each of the meridional and zonal directions. The divergence of these vertically integrated values was then calculated for the entire basin, the negative of which was the resulting atmospheric moisture convergence.

Tendencies of the precipitable water content ($\partial W/\partial t$) and terrestrial water storage ($\partial s/\partial t$) terms were calculated on a monthly basis. For example, the precipitable water tendency value for April resulted from the difference between the value of W for May and March, divided by ∂t of two months.

Evaporation was calculated by dividing surface latent heat flux (in watts per square metre) by the latent heat of vaporization of water (the temperature dependent values which are found in Rogers & Yau (1984)). This was necessary because the NARCCAP variable representing evaporation (surface evaporation of condensed water (evps)) was not published for each model. The calculated evaporation was compared with published evps values (when available) over ocean grid points and was found to be identical, confirming the validity of the evaporation calculation.

3 Results

In this section, various components of the atmospheric and terrestrial water balances, including absolute and relative residuals, are discussed. For the 1971–2000 base period the observed mean streamflow of the Churchill River is approximately 1825 $m^3\ s^{-1}$ (1.70 mm d^{-1}) (Water Survey of Canada, 2010), and the mean simulated runoff from all NARCCAP ensemble members used here is 1553 $m^3\ s^{-1}$ (1.44 mm d^{-1}), with a 90% uncertainty range of 1180 to 1927 $m^3\ s^{-1}$. Mean ensemble $P–E$ is 1618 $m^3\ s^{-1}$ (1.51 mm d^{-1}), with a 90% uncertainty range of 1062 to 2173 $m^3\ s^{-1}$.

Figure 2 shows base period ensemble member simulations and corresponding observations for precipitation and runoff. Monthly precipitation data were extracted from the Global Precipitation Climatology Centre's (GPCC) 0.5 degree resolution dataset (Meyer-Christoffer et al., 2011). The gridded GPCC data were checked using four corresponding Environment Canada in situ meteorological stations in, and around, the Churchill River basin and discrepancies in mean monthly values were found to be less than 0.2 mm d^{-1}.

Because approximately three-quarters of the runoff in the Churchill River basin occurs upstream of Churchill Falls hydroelectric facility, a direct comparison between simulated runoff and observed streamflow at the river's outlet would not be useful. Naturalized flow, which negates the effects of damming and water management, is preferred for model validation (Music & Caya, 2007). As such, Fig. 2 uses naturalized streamflow data, created by Fortin and Latraverse (2000), which accounts for the impact of the reservoirs and control structures of Churchill Falls. They approximated natural inflows into each reservoir (I_N) (i.e., runoff) by applying Eq. (3).

$$\frac{ds}{dt} = I_N + I_C - O_C. \quad (3)$$

Here, ds/dt is the change in reservoir storage, I_C is the controlled inflow into the reservoir (via control structures), and O_C is controlled outflow form the reservoir. Direct precipitation and evaporation over the reservoir are considered to be implicit in the measured ds/dt. The mean annual observed streamflow is 1825 $m^3\ s^{-1}$, and the mean annual naturalized streamflow is 1875 $m^3\ s^{-1}$. Observed streamflow is slightly lower because of the additional evaporation from the reservoirs. Both observed and naturalized flows can be seen in Fig. 2.

The observed precipitation and the naturalized flow both fell within the bounds of the ensemble's simulations, giving confidence that the simulations provide adequate representations of base period precipitation and runoff. The only exception was runoff simulated for November, December, and January, which was lower than the naturalized flow.

Figure 3 plots base period component breakdown of each ensemble member along with the atmospheric and terrestrial residuals. (Note that snow water equivalent (SWE) data were not available for the Hadley Regional Climate Model (HRM3)-Geophysical Fluid Dynamics Laboratory (GFDL) model, meaning it was impossible to calculate terrestrial water balance residuals.) From Fig. 3 it is apparent that the

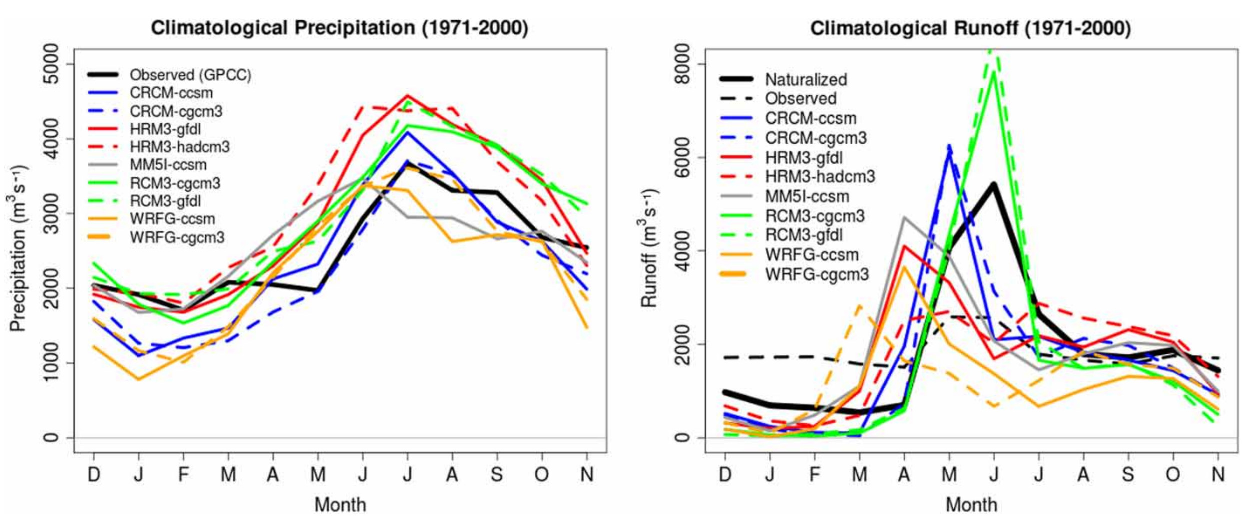

Fig. 2 Mean simulated precipitation (left panel) and runoff (right panel) compared with observations.

 http://dx.doi.org/10.1080/07055900.2015.1029870
La Société canadienne de météorologie et d'océanographie

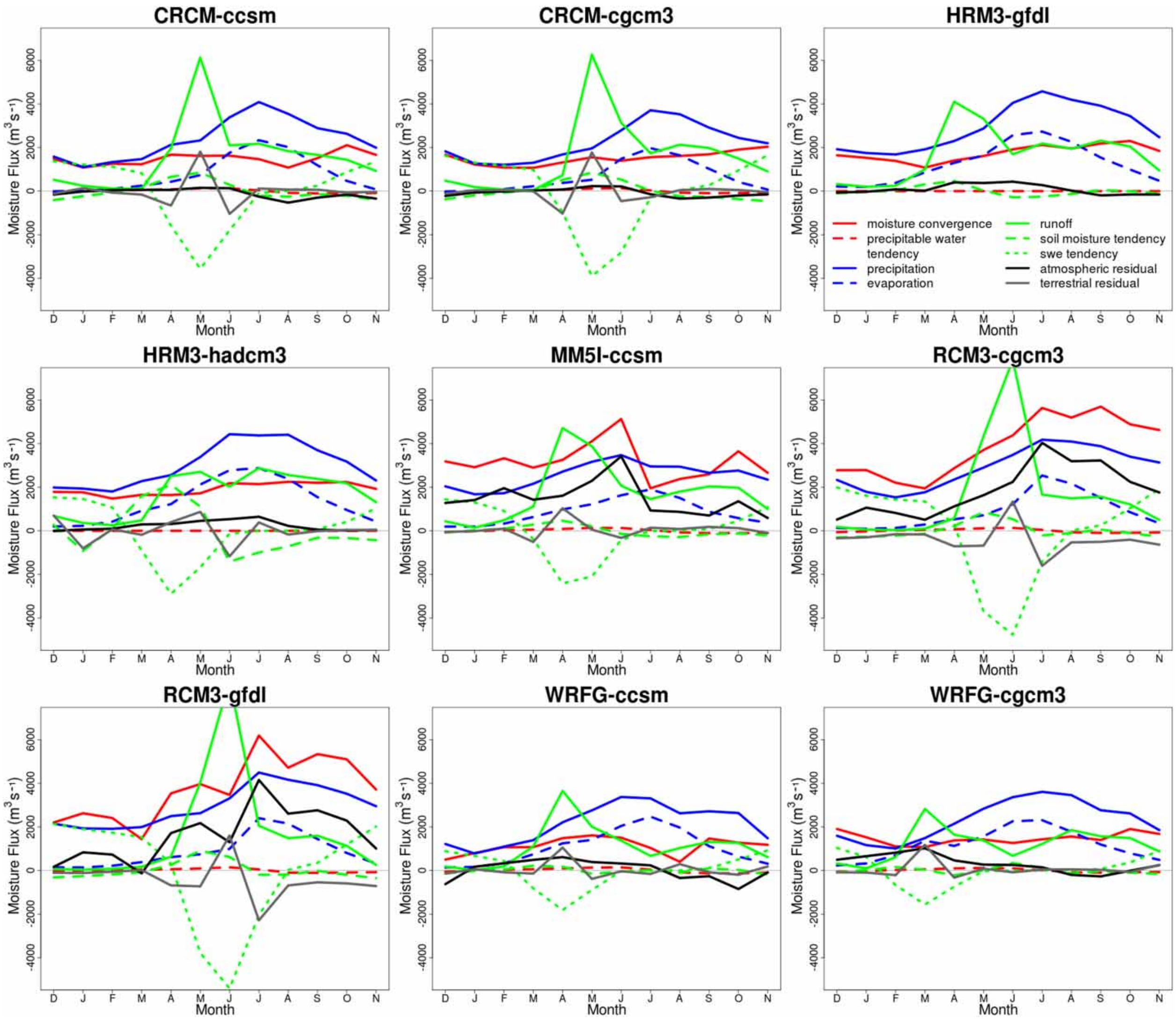

Fig. 3 Base period (1971–2000) water balance component breakdown.

precipitable water tendency (the change in precipitable water over time) contributes the least to the water balance from month to month. This is an expected result that has been found by others (Berbery & Rasmusson, 1999; Chen et al., 1996; Dimri, 2012). Similar results were found for the future period; however, the plot was omitted for space considerations.

Over the span of a year, precipitation contributes the most to each water balance (2602 $m^3 s^{-1}$ on average), except for the Regional Climate Model, version 3 (RCM3)-Third Generation Coupled Global Climate Model (CGCM3), RCM3-GFDL, and the Pennsylvania State University/National Center for Atmospheric Research Mesoscale Model 5 (MM5I)-Community Climate System Model (CCSM) where atmospheric moisture convergence dominates (with an average of 3595 $m^3 s^{-1}$). Noticeable spikes occur during spring runoff, which is a direct result of the spring melt's decrease in SWE stored on the land surface. Soil moisture also increases as the snowpack melts. The only ensemble member that does not follow this norm—runoff plateaus in April and remains high into the fall—is the HRM3-Hadley Centre Coupled Model, version 3 (HADCM3). Also, the amplitude of its soil moisture tendency is relatively high, with a root mean square (RMS) of 1043 $m^3 s^{-1}$, compared with other models that have an average RMS of 277 $m^3 s^{-1}$.

Moisture convergence is consistently positive throughout the year for all ensemble members, which indicates that the Churchill River basin is a moisture sink year round. Both precipitation and evaporation are highest in the summer for all ensemble members.

There are clear differences between ensemble members, the largest of which can be found in atmospheric moisture for which RCM3-CGCM3, RCM3-GFDL, and MM5I-CCSM are substantially higher than the bulk of the ensemble members (average of 3595 $m^3 s^{-1}$ compared with 1539 $m^3 s^{-1}$), especially in the summer and fall months.

Although some similarities and differences between moisture balance components for a given time period and ensemble member can be gleaned from the plots, a quantitative summary of the water balance residuals, as found in Tables 3 and 4, will provide more insight into the water balance closure.

a *Mean Annual Residuals*

The mean terrestrial water balance residual (ε_T) was always much less than the atmospheric residual (ε_A) for all models and time periods. The average magnitudes for the base period ε_T and ε_A were 122 and 647 $m^3 s^{-1}$, respectively, while for the future period they were 166 and 738 $m^3 s^{-1}$, respectively. The magnitudes of the future period ε_A were larger than those for the base period for five out of the seven models (HRM3-HADCM3 and MM5I-CCSM did not have sufficient data published at the time of analysis for water balance analyses), the exceptions being CRCM-CGCM3 and Weather Research and Forecasting Grell (WRFG)-CGCM3 model which, respectively, had base period ε_A magnitudes of 71 and 326 $m^3 s^{-1}$ and future period ε_A magnitudes of 35 and 281 $m^3 s^{-1}$. The magnitudes for ε_T from base to future periods increased in two-thirds of the models, while the remaining two models, CRCM-CGCM3 and WRFG-CGCM3, once again saw small decreases of 1 and 11 $m^3 s^{-1}$, respectively.

The CRCM and HRM3 ensemble members typically had the lowest mean residuals for both base and future periods (ranging from 35 to 229 $m^3 s^{-1}$ for ε_A and from 2 to 32 $m^3 s^{-1}$ for ε_T), while WRFG was only slightly larger (55 to 326 $m^3 s^{-1}$ for ε_A and from 29 to 63 $m^3 s^{-1}$ for ε_T). The RCM3 models consistently had the highest ε_A magnitudes (1616 to 2206 $m^3 s^{-1}$) and ε_T magnitudes (391 to 443 $m^3 s^{-1}$). The MM5I-CCSM ensemble member had a relatively high atmospheric residual of 1475 $m^3 s^{-1}$ but a relatively low terrestrial residual of 59 $m^3 s^{-1}$ (future period data for MM5I-CCSM were not published at the time of analysis).

For both time periods, CRCM ensemble members had an overall negative mean ε_A, indicating that $P–E$ was typically greater than the contributions of the atmospheric moisture convergence and the precipitable water tendency. All other ensemble members had overall positive mean ε_A, though 27% of months for WRFG models and 46% of months for HRM3-GFDL showed negative residuals. Both RCM3 ensemble members had negative mean terrestrial water balance residuals for both time periods (ranging from −391 to −443 $m^3 s^{-1}$), meaning that $P–E$ was typically greater than the combined contributions of runoff and the terrestrial water storage terms. The other models tended to be on the positive side (though close to zero), with the exception of future period CRCM-CCSM (−32 $m^3 s^{-1}$).

b *Annual Cycle of Residuals*

In the discussion of the annual cycle, the root mean square residual (RSMR) gives a better idea of the magnitude of variations from zero than the means of ε_A and ε_T for each

TABLE 3. Base period atmospheric and terrestrial water balance residual values for all available ensemble members.

		BASE PERIOD (1971–2000)									
		CRCM CCSM	CRCM CGCM3	HRM3 GFDL	HRM3 HADCM3	MM5I CCSM	RCM3 CGCM3	RCM3 GFDL	WRFG CCSM	WRFG CGCM3	RMSR
Atmospheric Residual ($m^3 s^{-1}$)	Dec.	−109	−96	−100	21	1314	648	28	−240	638	**542**
	Jan.	1	−12	−30	60	1450	1119	839	194	701	**714**
	Feb.	−2	−50	81	97	1910	783	693	274	774	**777**
	Mar.	−35	−46	20	294	1313	419	−209	363	943	**583**
	Apr.	−103	−58	399	313	1432	976	1595	426	288	**822**
	May	−98	−4	371	455	2025	1402	1987	121	21	**1074**
	Jun.	−127	−44	431	534	3157	1980	1006	36	38	**1308**
	Jul.	−320	−213	273	643	862	3949	4044	153	100	**1925**
	Aug.	−365	−194	23	225	1016	3327	2798	−171	−23	**1498**
	Sep.	−85	−107	−198	51	915	3417	2976	−5	−140	**1544**
	Oct.	44	−33	−155	18	1571	2431	2470	−593	133	**1286**
	Nov.	−164	−1	−147	41	737	1846	1167	104	443	**787**
	MEAN	**−114**	**−71**	**81**	**229**	**1475**	**1858**	**1616**	**55**	**326**	**968**
	RMSR	**164**	**98**	**235**	**311**	**1606**	**2179**	**2025**	**276**	**476**	**1151**
Terrestrial Residual ($m^3 s^{-1}$)	Dec.	−139	−113	N/A	706	−53	−337	−108	−152	−35	**292**
	Jan.	134	37	N/A	−805	−14	−301	−112	58	−69	**312**
	Feb.	−69	50	N/A	68	99	−156	−59	−83	−207	**112**
	Mar.	−159	−6	N/A	−184	−512	−170	20	−139	1135	**455**
	Apr.	−664	−1029	N/A	396	1034	−711	−683	1049	−389	**787**
	May	1812	1771	N/A	868	53	−681	−725	−386	50	**1020**
	Jun.	−1044	−460	N/A	−1172	−326	1341	1606	−35	−147	**947**
	Jul.	118	−282	N/A	383	139	−1606	−2287	−157	−19	**1006**
	Aug.	70	43	N/A	−172	85	−531	−685	290	−2	**331**
	Sep.	66	99	N/A	−15	179	−506	−540	−82	61	**275**
	Oct.	−72	51	N/A	43	125	−407	−591	−194	67	**270**
	Nov.	−30	−41	N/A	40	−97	−630	−711	183	309	**361**
	MEAN	**2**	**10**	**N/A**	**13**	**59**	**−391**	**−406**	**29**	**63**	**202**
	RMSR	**640**	**614**	**N/A**	**551**	**358**	**747**	**933**	**352**	**367**	**603**

TABLE 4. Future period atmospheric and terrestrial water balance residual values for all available ensemble members.

		FUTURE PERIOD (2041–2070)									
		CRCM CCSM	CRCM CGCM3	HRM3 GFDL	HRM3 HADCM3	MM5I CCSM	RCM3 CGCM3	RCM3 GFDL	WRFG CCSM	WRFG CGCM3	RMSR
Atmospheric Residual ($m^3 s^{-1}$)	Dec.	−95	41	−117	N/A	N/A	1038	837	427	769	**607**
	Jan.	−61	−17	−26	N/A	N/A	530	684	536	782	**486**
	Feb.	−58	−60	38	N/A	N/A	681	672	541	907	**540**
	Mar.	−18	−15	201	N/A	N/A	676	706	625	740	**526**
	Apr.	−56	−45	296	N/A	N/A	1062	582	327	373	**508**
	May	−204	−38	340	N/A	N/A	1734	1324	53	34	**839**
	Jun.	−181	−120	426	N/A	N/A	3934	2773	297	−183	**1833**
	Jul.	−527	−84	556	N/A	N/A	4387	4557	17	−118	**2409**
	Aug.	−421	−79	−69	N/A	N/A	3134	4105	−58	−176	**1960**
	Sep.	−166	−26	−118	N/A	N/A	4429	4159	−199	52	**2299**
	Oct.	−322	−92	−153	N/A	N/A	2790	3692	−150	−75	**1756**
	Nov.	−2	116	−195	N/A	N/A	2079	1544	381	266	**998**
	MEAN	**−176**	**−35**	**98**	**N/A**	**N/A**	**2206**	**2136**	**233**	**281**	**1171**
	RMSR	**238**	**70**	**263**	**N/A**	**N/A**	**2625**	**2627**	**361**	**489**	**1429**
Terrestrial Residual ($m^3 s^{-1}$)	Dec.	−90	7	N/A	N/A	N/A	−364	−314	20	−31	**200**
	Jan.	151	−33	N/A	N/A	N/A	−239	−240	95	−121	**164**
	Feb.	−305	50	N/A	N/A	N/A	−320	−204	−206	−111	**222**
	Mar.	−356	−205	N/A	N/A	N/A	−217	−198	−67	854	**406**
	Apr.	286	−807	N/A	N/A	N/A	−1109	−754	890	−153	**747**
	May	812	2031	N/A	N/A	N/A	557	−129	−233	156	**930**
	Jun.	−490	−995	N/A	N/A	N/A	−497	76	−183	−391	**527**
	Jul.	−116	53	N/A	N/A	N/A	−802	−1289	−91	650	**677**
	Aug.	−70	56	N/A	N/A	N/A	−389	−976	495	−390	**501**
	Sep.	35	−120	N/A	N/A	N/A	−552	−532	−307	48	**341**
	Oct.	−194	173	N/A	N/A	N/A	−457	−327	47	350	**291**
	Nov.	−45	−105	N/A	N/A	N/A	−604	−428	50	−238	**321**
	MEAN	**−32**	**9**	**N/A**	**N/A**	**N/A**	**−416**	**−443**	**43**	**52**	**250**
	RMSR	**328**	**700**	**N/A**	**N/A**	**N/A**	**563**	**578**	**328**	**378**	**500**

ensemble member throughout the year (RMSR rows in Tables 3 and 4) and across the entire ensemble for each month (RMSR columns).

The WRFG and MM5I ensemble members had the lowest overall terrestrial RMSR for both time periods, and CRCM-CCSM had an equally low RMSR for the future period (from 328 to 378 $m^3 s^{-1}$). The RCM3-CGCM3 and RCM3-GFDL ensemble members had the highest overall terrestrial RMSR for the base period (747 and 933 $m^3 s^{-1}$, respectively) while CRCM-CGCM3 had the highest for the future period (700 $m^3 s^{-1}$). The RCM3 members had the highest overall atmospheric RMSR for both time periods (2025 to 2627 $m^3 s^{-1}$), while MM5I-CCSM was a distant second for the base period (1606 $m^3 s^{-1}$). The CRCM-CCSM and CRCM-CGCM3 ensemble members had the lowest atmospheric RMSR for both time periods (70 to 238 $m^3 s^{-1}$).

Whether the terrestrial or atmospheric RMSR was larger depended on the time period in question and on individual ensemble members. Overall 57% of the simulations had a larger atmospheric RMSR than terrestrial.

The low mean annual ε_T and high terrestrial RMSR for the CRCM ensemble members means that the month-to-month residuals almost cancel each other over the span of a year, but there are substantial residuals when examining individual months, especially during the spring melt (on the order of 2000 $m^3 s^{-1}$). A similar, but less severe, situation occurs in the WRFG and MM5I ensemble members (around 1000 $m^3 s^{-1}$).

The highest atmospheric RMSR for both time periods occurred in July (1925 and 2409 $m^3 s^{-1}$), though the RMSR for September was similar for the future period (2299 $m^3 s^{-1}$). The lowest RMSRs (between 486 and 839 $m^3 s^{-1}$) occurred in the winter and early spring months. The highest terrestrial RMSR for both time periods (1020 and 930 $m^3 s^{-1}$) occurred in May, but July was a close second for the base period (1006 $m^3 s^{-1}$). The lowest RMSR for the base period (112 $m^3 s^{-1}$) occurred in February, while the lowest for the future period (164 $m^3 s^{-1}$) occurred in January. Periods with large ε_A correspond with those summers when atmospheric moisture transport, precipitation, and evaporation are highest, while large ε_T corresponds with the transition period of the spring melt.

c *Relative Residuals*

Table 5 presents the mean atmospheric and terrestrial water balance residuals relative to simulated climatological P–E values. The magnitudes of the atmospheric residuals range from −10.1 to 102.8%, while the terrestrial residuals range from −19.5 to 5.5%.

There is a very high correlation between the relative magnitudes of the residuals between the base and future periods for each ensemble member (Pearson's $r = 0.99$). All CRCM and HRM3 relative residuals as well as WRFG and RCM3 relative

TABLE 5. Atmospheric and terrestrial residuals relative to climatological *P–E* for base and future periods, as well as *P–E* climate change signal $\Delta\,(P-E)$.

		CRCM CCSM	CRCM CGCM3	HRM3 GFDL	HRM3 HADCM3	MM5I CCSM	RCM3 CGCM3	RCM3 GFDL	WRFG CCSM	WRFG CGCM3
1971–2000	$P-E$ (m^3 s^{-1})	1592	1583	1663	1687	1684	2028	2091	1084	1147
	ε_A (%)	−7.2	−4.5	4.9	13.6	87.6	91.6	77.3	5.1	28.4
	ε_T (%)	0.1	0.6	N/A	0.8	3.5	−19.3	−19.4	2.7	5.5
2041–2070	$P-E$ (m^3 s^{-1})	1739	1761	1761	N/A	N/A	2145	2272	1242	1377
	ε_A (%)	−10.1	−2.0	5.6	N/A	N/A	102.8	94.0	18.8	20.4
	ε_T (%)	−1.8	0.5	N/A	N/A	N/A	−19.4	−19.5	3.5	3.8
$\Delta(P-E)$ (%)		9.2	11.2	5.9	N/A	N/A	5.8	8.7	14.6	20.1

terrestrial residuals are consistent between time periods to within three percentage points. This indicates the residuals are systemic. The primary exceptions are WRFG's atmospheric residuals, which change from 5.1 to 18.8% and from 28.4 to 20.4%. RCM3's relative atmospheric residuals have similar percentage point changes, though consistency between time periods can still be inferred because of the much larger size of their relative residual magnitudes compared with those of WRFG (average of 91.4% compared with 18.2%, respectively). This is beneficial for climate change analyses because it is still possible to gain insight from the differences between base and future periods, even if the residuals are larger than the climate change signal (which is the case for several ensemble members).

The climate change signal for *P–E* ranges from 5.8 to 20.1%, with a mean increase of 8.6%. For a detailed look at the climate change signal of NARCCAP's models over the Churchill River basin see Roberts and Snelgrove (2015).

4 Discussion

Now that the atmospheric and terrestrial water balance residuals have been identified, this section will shed some light on the sources of imbalance in the current study. As discussed in the literature review, there are many possibilities including choice of sampling frequency, coordinate system, post-processing, model processes, and parameterizations. The impact of each of these will vary and is quantified when possible.

a *Sampling Frequency*

Published precipitation, evaporation, and runoff data are averages over a 3-hour time step (so 3-hour totals can easily be found), whereas specific humidity, wind components, precipitable water content, SWE, and soil moisture are instantaneous values. The 3-hour sampling frequency of the RCMs in this study was adequate for capturing the diurnal cycle for all averaged and instantaneous variables (Chen et al., 1996; Roads et al., 1998); however, there is some imbalance introduced when sampling instantaneous variables. This is especially true for atmospheric moisture convergence, which is the result of multiplying one instantaneous variable (specific humidity) by others (meridional and zonal wind components). That being said, the sampling frequency was the same for RCM3 as it was for other models and both RCM3 ensemble members experienced relatively similar and anomalously large budget residuals for both the base period (91.6 and 77.3%) and the future period (102.8 and 94.0%) (as did NCEP driven runs, Fig. 4, 105.6%). One would expect the non-linear impact of sampling to be considerably different across ensemble members, even if they employ the same RCM. As such, it is unlikely that sampling frequency contributed substantially to water balance residuals, especially ε_T. In order to isolate the impact of sampling frequency, cumulative atmospheric moisture convergence values for each time step would be needed in addition to the instantaneous values.

b *Coordinate Systems and Post-Processing*

All ensemble members operate in their own native coordinate systems (see Table 1), but published NARCCAP data have all been interpolated to a common set of pressure levels (by the respective modelling groups) for the sake of data consistency. Published precipitable water values are calculated within each model's native vertical coordinate system. As such, by comparing the manual calculation of precipitable water (from specific humidity at each pressure level) with published values (calculated in a model's native coordinates) the residual introduced to a single variable by converting to NARCCAP's pressure levels and undertaking a vertical integration can be quantified. The range of these results, calculated using Eq. (4), can be found in Table 6.

$$\varepsilon_{\text{relative}} = \left(\frac{W_{\text{published}} - W_{\text{calculated}}}{W_{\text{published}}}\right) \times 100\% \qquad (4)$$

This effect would be compounded when investigating moisture convergence because the specific humidity must be multiplied by wind at each level (meaning the values in Table 6 are conservative estimates). The mean values are relatively consistent for each RCM regardless of the forcing GCM or the time period, implying that these residuals are systemic. By considering the range of relative residuals the potential contribution of conversion to pressure levels and vertical integration can be appreciated. Minimum and maximum values refer to residuals from individual 3-hour time steps, whereas the mean spans the 30-year climatology. Some of the more extreme relative residuals were found when a precipitable water value (be it published or calculated) was anomalously small.

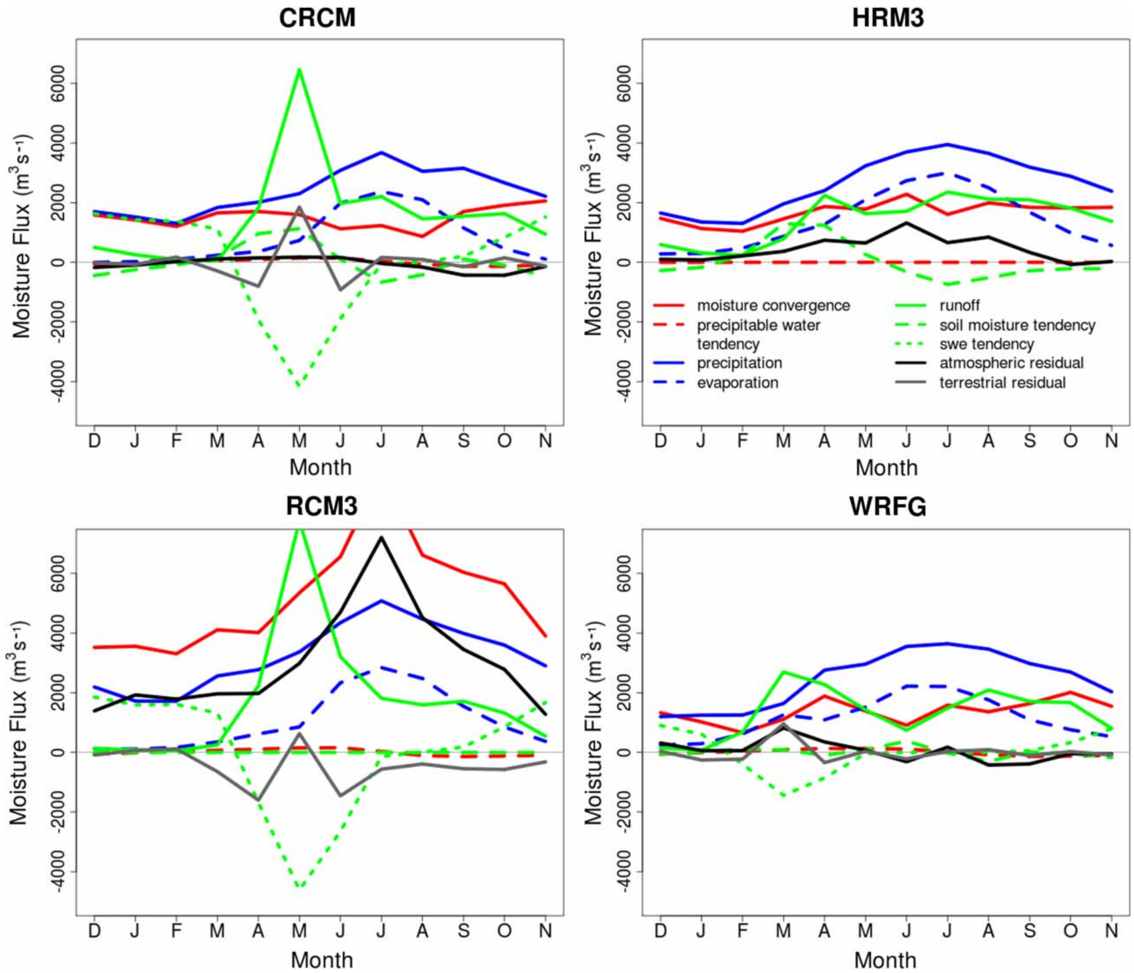

Fig. 4 RCM water balance component breakdown (1980–2004) driven by NCEP Reanalysis II.

TABLE 6. Range of relative residuals ($\varepsilon_{\text{relative}}$) resulting from conversion to pressure levels and the subsequent vertical integration.

		CRCM CCSM	CRCM CGCM3	HRM3 GFDL	HRM3 HADCM3	WRFG CCSM	WRFG CGCM3
1971–2000	Min. (%)	−6.7	−11.3	−29.9	−27.2	N/A[a]	−15.5
	Mean (%)	8.0	8.3	7.3	5.1	0.5	0.9
	Max. (%)	28.0	28.5	23.2	30.1	82.4	14.3
2041–2070	Min. (%)	−7.4	−10.4	−37.4	N/A	−60.5	−12.3
	Mean (%)	8.0	8.4	7.2	N/A	1.1	1.0
	Max. (%)	38.2	28.6	24.2	N/A	18.1	7.3

[a]This value was not available because some precipitable water values were published as zero (an unrealistic value), resulting in an infinite residual.

Unfortunately, published precipitable water data were not available for RCM3 or MM5I. Manual vertical integration was used to derive their precipitable water tendencies for the water balances of Eq. (1). Comparing tendencies calculated using published precipitable water data with those derived from manual vertical integration of other ensemble members showed this contributed on the order of 1% to precipitable water tendency values and made no substantial contribution to the overall residuals.

On a climatological basis, mean annual residuals have a smaller magnitude than month-to-month values. During analysis, the time frame over which soil moisture, SWE, and precipitable water tendencies were calculated was found to have an impact on the magnitude of the month-to-month residuals, predominantly with SWE tendency during the spring melt. The storage tendency terms were calculated with a ∂t of two months, as represented in seconds (on average, 5,256,000 seconds per two months). If the tendency calculation was performed with a ∂t of one month (i.e., if April's value was the difference between April and March or the difference between May and April) then the magnitude of the storage tendency terms would be different. The effect of this evens out over the span of a year and did not substantially affect mean or RMS residuals.

Residuals at the 3-hour time interval of published data were also calculated and found to be almost identical to the mean annual residuals found above (< 1% difference) despite varying widely from time step to time step. The annual cycles of 3-hour residuals followed the same patterns as monthly residuals.

c *Modelling Processes and Parameterization Schemes*

Labrador has a precipitation recycling ratio (i.e., the percentage of precipitation that originates from local evaporation) of roughly 6 to 9%, and a high recycling ratio is considered to be greater than 20% (Trenberth, 1998). Evidence of this can be found in Fig. 3 where both atmospheric moisture convergence and land-surface evaporation play a significant role. A high recycling ratio implies atmospheric water balances are strongly influenced by parameterizations because of the increased role of evapotranspiration and land-surface schemes. Conversely, a low recycling ratio implies atmospheric water balances are more strongly influenced by model dynamics (i.e., resolved moisture convergence). The Churchill River basin's mid-range recycling ratio implies that atmospheric water balances are influenced relatively equally by parameterizations and dynamical processes. Large-scale moisture advection is the only water balance process that is adequately resolved in most ensemble members. As such, parameterization is required to represent the unresolved processes (e.g., turbulence, convection, evaporation, condensation, and radiative fluxes) with impacts on the water budgets that vary depending on the respective schemes. Some parameterization schemes allow a certain amount of water to be lost within specified accuracy limits (e.g., the Canadian Land Surface Scheme (CLASS) used in the CRCM has an accuracy limit of 1×10^{-3} kg m^{-2} (0.001 mm) per time step (Verseghy, 2009)). More examples of variation in evaporation and soil moisture schemes have been found by others (see literature review). The fallibility of parameterizations is further evidenced by unrealistic output values found in NARCCAP data, such as negative runoff and zero precipitable water content.

For a comparison of the isolated effects of the RCMs for which the driving model is consistent across all models, Fig. 4 presents the water balance component breakdown for four of NARCCAP's RCMs driven by NCEP Reanalysis II (Kanamitsu et al., 2002), for the 1980–2003 period (there were insufficient MM5I data and no HRM3 SWE data available for analysis). Table 7 explicitly lists the corresponding residuals. The differences in residuals between models emphasizes the role that individual RCMs and their respective coordinate systems, parameterizations, and modelling processes play in atmospheric and terrestrial water balances. There are strong similarities between the water balance components and residuals in Fig. 4 and those in Fig. 3 for each RCM, confirming the dominant role of the RCM over the forcing model.

d *Geographical Considerations*

The influence of regional variation and basin size are also worth discussing. Dimri (2012) found that a similar version of RCM3-NCEP had a much smaller water budget residual over the western Himalayas, despite the complex terrain, than was found over the Churchill River basin. Their study region was over 3.5 times larger, and they investigated a rectangular domain because they were not interested in a single basin. Music and Caya (2007) studied a similar version of CRCM-NCEP over the Mississippi River basin (3.2×10^6 km^2) and found that their water balance residuals followed a similar annual cycle to those in Fig. 4 (with largest positive ε_A occurring in late spring and largest negative ε_A in autumn), though they had a consistently smaller magnitude. The largest monthly ε_A was approximately 0.2 mm d^{-1} compared with 0.4 mm d^{-1} found here. (A previous version of CRCM had larger mean annual and monthly imbalances. This was

TABLE 7. Atmospheric and terrestrial water balance residual values for all available models driven by NCEP Reanalysis II.

		NCEP (1980–2003)									
		CRCM	HRM3	RCM3	WRFG	RMSR			CRCM	RCM3	WRFG	RMSR
Atmospheric Residual (m^3 s^{-1})	Dec.	−173	103	1390	314	720	Terrestrial Residual (m^3 s^{-1})	Dec.	−20	−85	36	54
	Jan.	−96	77	1927	59	966		Jan.	−70	63	−256	158
	Feb.	20	215	1786	59	900		Feb.	172	116	−229	178
	Mar.	112	365	1963	818	1080		Mar.	−291	−647	958	688
	Apr.	147	739	1974	349	1071		Apr.	−806	−1604	−344	1055
	May	172	646	2983	72	1529		May	1853	628	35	1130
	Jun.	163	1318	4702	−314	2448		Jun.	−925	−1458	−218	1005
	Jul.	−38	658	7206	174	3619		Jul.	162	−563	29	339
	Aug.	−162	843	4516	−426	2308		Aug.	94	−392	89	238
	Sep.	−433	331	3454	−388	1759		Sep.	−151	−550	−108	335
	Oct.	−436	−74	2782	−46	1409		Oct.	150	−573	25	342
	Nov.	−142	25	1276	−54	643		Nov.	−128	−319	−82	204
	MEAN	−72	437	2997	51	1515		MEAN	3	−449	−6	259
	RMSR	215	588	3430	338	1752		RMSR	655	749	320	604

mitigated in the current version by an adjustment applied to specific humidity values at each grid point.)

Another geographical consideration is that the Churchill River basin is near the eastern lateral boundary of the NARCCAP domain. Because the basin lies in a predominantly westerly atmospheric flow it is near the outflow region of each of the RCMs. This relative proximity to the lateral boundary may be introducing residual, particularly in the atmospheric water balance. It has been found that the outflow region in limited area models, such as RCMS, can exhibit physically inconsistent behaviour because of the requirement for the RCM data to align with that of the forcing GCM (Lucarini, Danihlik, Kriegerova, & Speranza, 2007; Marbaix, Gallee, Brasseur, & van Ypersele, 2003). This alignment occurs in the buffer zone where moisture imbalances are common and may result in numerical errors bouncing back into the RCM domain (Liang, Kunkel, & Samel, 2001).

e *Various*

While condensed moisture (e.g., as clouds) is not included in the specific humidity or precipitable water variables used in this analysis, the contribution it makes is typically small (on the order of 1%). A similar argument can be made for sources of terrestrial water storage other than soil moisture and snow pack (e.g., canopy interception).

The only RCM in the current ensemble that used spectral nudging (pushing variable values closer to those found in the driving GCM) was CRCM and, as shown in Table 3, both CRCM ensemble members had relatively low residuals. It should not be assumed that spectral nudging implies a smaller residual because the onus of water balance closure is then shifted to the driving GCM, which is not guaranteed to be more physically consistent than the RCM. That being said, GCMs do not need to accommodate prescribed lateral boundaries and their respective buffer zones, discussed above. More insight will be gained once simulation results are published for the Experimental Climate Prediction Center Regional Spectral Model (ECP2; another NARCCAP RCM), which also uses spectral nudging.

f *Primary Contributors to Moisture Imbalance*

Based on the above analysis, there are three primary factors of comparable importance that contributed to residuals being introduced into the water balances. (Because none of these contributions were able to be quantified, they are not listed in order of importance.) The first is geographical considerations, particularly the proximity of the study region to the RCM's outflow lateral buffer zone. The second is the interpolation to NARCCAP's standard pressure levels from each RCM's native vertical coordinate system and subsequent vertical interpolation using these pressure level data. The third is the various model parameterizations and processes, including land-surface schemes.

There were several other potential contributing factors discussed above, though they were found to have a non-substantial effect on the water balance residuals. These included the 3-hour sampling frequency of the RCMs, sources of moisture not included in the water balance calculations (e.g., clouds), and the various calculations performed (other than the aforementioned vertical integration of pressure levels), especially averaged over the full year.

5 Summary and conclusions

Mean annual atmospheric and terrestrial water balance residuals were quantified as were their mean annual cycles. The atmospheric water balance residuals were consistently higher than the terrestrial residuals, regardless of time period or ensemble member. Some of this difference can be attributed to the residual resulting from the interpolation of atmospheric data to pressure levels and its subsequent integration, found in Table 6.

With regard to the annual cycle, the winter and early spring months had the lowest overall RMSRs. The highest atmospheric RMSR occurred in mid- to late summer, while the highest terrestrial RMSR occurred during the spring melt. There was no pattern across time periods or ensemble members that indicated whether terrestrial or atmospheric RMSR was the highest.

Water balance residuals were found to be much more consistent between common RCMs than common GCMs. This implies that residuals are largely a function of RCM and not the driving GCM. Similarly, water balance residuals have been found to be predominantly systemic, implying that anomalies (including interannual variation and the climate signal) are better represented than individual field values.

Although it was not feasible to isolate all root causes of the atmospheric and terrestrial water cycle imbalances, this study was able to explore or quantify some causes and eliminate others. At this point, it would be premature to rank the models for physical consistency because the investigation needs to expand to include additional regions of varying climatologies and sizes. This can be accomplished by expanding the boundaries of the Churchill River basin to cover an area greater than 2×10^5 km^2 and comparing the results with those found here and with an equally sized region (elsewhere in North America) modelled by NARCCAP.

Expanding the geographic focus would also be useful in determining the impact of basin proximity to the lateral buffer zone of each RCM. Until such a comparison is undertaken it must not be assumed that residuals found here would occur in every region of the NARCCAP domain with the same magnitudes. This is especially true for atmospheric water balances because the large-scale circulation of an RCM is more directly influenced by the forcing model (and buffer zone) than the terrestrial water balance components. As such, the terrestrial water balance residuals (relative to other water balance components, as in Table 5) are more likely to be applicable to other regions.

Additional sources of uncertainty that merit further investigation include the impacts of the choice of vertical coordinate system (plus vertical coordinate discrepancies between RCM and GCM), parameterization scheme choices, and spectral nudging. Detailed investigation of individual parameterization schemes and dynamic processes is beyond the scope of this paper and would be most effectively investigated by individual modelling teams.

One recommendation that should be incorporated in future ensemble studies is to publish accumulated moisture convergence fields calculated using an RCM's native vertical coordinate system. This would provide a consistent variable across all ensemble members without the additional residual introduced by converting to, and performing calculations in, a pressure level coordinate system (not to mention drastically reduce the amount of data to download and store).

Although NARCCAP's ensemble is imperfect (as are all simulations), it is still able to provide much useful information, particularly about the impacts of climate change. Water balance errors were found to be largely systemic, meaning that anomalies and changes over time (e.g., under climate change) are more reliable than individual field values (Berbery & Rasmusson, 1999; Trenberth, 1991). Even if atmospheric and terrestrial water balance residuals exist, models still provide useful information about a basin's moisture flux (Liu & Stewart, 2003). Additionally, long-term average moisture convergence and $P–E$ should equal long-term average runoff, providing insight for practical applications such as water resource management, as investigated by Roberts and Snelgrove (2015).

Acknowledgements

This work would not have been possible without the generous financial support of Nalcor Energy Inc, the Natural Sciences and Engineering Research Council (NSERC), Mitacs, and TD Canada Trust.

We wish to thank the North American Regional Climate Change Assessment Program (NARCCAP) for providing access to the data used in this paper; NARCCAP is funded by the National Science Foundation, the U.S. Department of Energy, the National Oceanic and Atmospheric Administration, and the U.S. Environmental Protection Agency Office of Research and Development.

Disclosure statement

No potential conflict of interest was reported by the authors.

References

Berbery, E. H., & Rasmusson, E. M. (1999). Mississippi moisture budgets on regional scales. *Monthly Weather Review*, *127*, 2654–2673. doi:10.1175/1520-0493(1999)127<2654:MMBORS>

Caya, D., & Laprise, R. (1999). A semi-implicit semi-Lagrangian regional climate model: The Canadian RCM. *Monthly Weather Review*, *127*(3), 341–362. doi:10.1175/1520-0493(1999)127<0341:ASISLR>

Chahine, M. T. (1992). The hydrological cycle and its influence on climate. *Nature*, *359*, 373–380. doi:10.1038/359373a0

Chen, S.-C., Norris, C., & Roads, J. (1996). Balancing the atmospheric hydrologic budget. *Journal of Geophysical Research*, *101*, 7341–7358. doi:10.1029/95JD01746

Collins, W. D., Bitz, C. M., Blackmon, M. L., Bonan, G. B., Bretherton, C. S., Carton, J. A., … Smith, R. D. (2006). The community climate system model version 3 (CCSM3). *Journal of Climate*, *19*(11), 2122–2143. doi:10.1175/JCLI3761.1

Dimri, A. (2012). Atmospheric water budget over the western Himalayas in a regional climate model. *Journal of Earth System Science*, *121*(4), 963–973. doi:10.1007/s12040-012-0204-8

Environment Canada. (2014). *Historical climate data* [Data]. Retrieved from http://climate.weather.gc.ca/

Flato, G. M. (2005). The Third Generation Coupled Global Climate Model (CGCM3). *Environment Canada Canadian Centre for Climate Modelling and Analysis note*. Retrieved from http://www.ec.gc.ca/ccmac-cccma/default.asp?n=1299529F-1

Fortin, V., & Latraverse, M. (2000). Une base de données hydrométéorologiques pour le développement d'un indicateur d'hydraulicité. *Logiciels de réseaux Technologies de transport et de distribution (IREQ-2000-268)*, Quebec, Canada.

GFDL Global Atmospheric Model Development Team. (2004). The new GFDL global atmospheric and land model AM2-LM2: Evaluation with prescribed SST simulations. *Journal of Climate*, *17*, 4641–4673. doi:10.1175/JCLI-3223.1

Giorgi, F., Marinucci, M. R., & Bates, G. T. (1993a). Development of a second-generation regional climate model (RegCM2). Part I: Boundary-layer and radiative transfer processes. *Monthly Weather Review*, *121*(10), 2794–2813. doi:10.1175/1520-0493(1993)121<2794:DOASGR>

Giorgi, F., Marinucci, M. R., Bates, G. T., & De Canio, G. (1993b). Development of a second-generation regional climate model (RegCM2). Part II: Convective processes and assimilation of lateral boundary conditions. *Monthly Weather Review*, *121*(10), 2814–2832. doi:10.1175/1520-0493(1993)121<2814:DOASGR>

Gordon, C., Cooper, C., Senior, C. A., Banks, H., Gregory, J. M., Johns, T. C. … Wood, R. A. (2000). The simulation of SST, sea ice extents and ocean heat transports in a version of the Hadley Centre coupled model without flux adjustments. *Climate Dynamics*, *16*(2–3), 147–168. doi:10.1007/s003820050010

Grell, G. A., Dudhia, J., & Stauffer, D. R. (1993). A description of the fifth generation Penn State/NCAR Mesoscale Model (MM5). *NCAR Technical Note NCAR/ TN-398*. Boulder, CO: NCAR.

Hack, J. J., Kiehl, J. T., & Hurrell, J. W. (1998). The hydrologic cycle and thermodynamic characteristics of the NCAR CCM3. *Journal of Climate*, *11*(6), 1179–1206. doi:10.1175/1520-0442(1998)011<1179:THATCO>

Hirschi, M., Seneviratne, S. I., & Schär, C. (2006). Seasonal variations in terrestrial water storage for major midlatitude river basins. *Journal of Hydrometeorology*, *7*(1), 39–60. doi:10.1175/JHM480.1

Hu, H., Oglesby, R. J., & Marshall, S. (2005). The simulation of moisture processes in climate models and climate sensitivity. *Journal of Climate*, *18*(13), 2172–2193. doi:10.1175/JCLI3384.1

IPCC. [Nakicenovik, N., & Swart, R. (Eds.)]. (2000). *Emissions scenarios*. Cambridge, UK: Cambridge University Press.

Jin, F., & Zangvil, A. (2010). Relationship between moisture budget components over the eastern Mediterranean. *International Journal of Climatology*, *30*(5), 733–742. doi:10.1002/joc.1911

Jones, R., Hassell, D., Hudson, D., Wilson, S., Jenkins, G., & Mitchell, J. (2004). *Generating high resolution climate change scenarios using PRECIS*. Exeter: Met Office Hadley Centre.

Kanamitsu, M., Ebisuzaki, W., Woollen, J., Yang, S. K., Hnilo, J. J., Fiorino, M., & Potter, G. L. (2002). NCEP-DOE AMIP-II Reanalysis (R-2). *Bulletin* *of the American Meteorological Society*, *83*(11), 1631–1643. doi:10.1175/BAMS-83-11-1631

Liang, X.-Z., Kunkel, K. E., & Samel, A. N. (2001). Development of a regional climate model for U.S. Midwest applications. Part 1: Sensitivity to buffer zone treatment. *Journal of Climate*, *14*, 4363–4378. doi:10.1175/1520-0442(2001)014<4363:DOARCM>2.0.CO;2

Liu, J., & Stewart, R. (2003). Water vapor fluxes over the Saskatchewan River Basin. *Journal of Hydrometeorology*, *4*, 944–959. doi:10.1175/1525-7541(2003)004<0944:WVFOTS>

Lucarini, V., Danihlik, R., Kriegerova, I., & Speranza, A. (2007). Does the Danube exist? Versions of reality given by various regional climate models and climatological data sets. *Journal of Geophysical Research: Atmospheres*, *112*, 1–17. D13103. doi:10.1029/2006JD008360

Marbaix, P., Gallee, H., Brasseur, O., & van Ypersele, J.-P. (2003). Lateral boundary conditions in regional climate models: A detailed study of the relaxation procedure. *Monthly Weather Review*, *131*, 461–479. doi:10.1175/1520-0493(2003)131<0461:LBCIRC>2.0.CO;2

Mearns, L. O., Gutowski, W., Jones, R., Leung, R., McGinnis, S., Nunes, A., & Qian, Y. (2009). A regional climate change assessment program for North America. *Eos, Transactions American Geophysical Union*, *90*(36), 311–311. doi:10.1029/2009EO360002

Meyer-Christoffer, A., Becker, A., Finger, P., Rudolf, B., Schneider, U., & Ziese, M. (2011). GPCC climatology version 2011 at 0.5°: Monthly land-surface precipitation climatology for every month and the total year from rain-gauges built on GTS-based and historic data [Data]. doi:10.5676/DWD_GPCC/CLIM_M_V2011_050

Min, W., & Schubert, S. (1997). The climate signal in regional moisture fluxes: A comparison of three global data assimilation products. *Journal of Climate*, *10*(10), 2623–2642. doi:10.1175/1520-0442(1997)010<2623:TCSIRM>

Mueller, B., Hirschi, M., & Seneviratne, S. I. (2011). New diagnostic estimates of variations in terrestrial water storage based on ERA-interim data. *Hydrological Processes*, *25*(7), 996–1008. doi:10.1002/hyp.7652

Music, B., & Caya, D. (2007). Evaluation of the hydrological cycle over the Mississippi River basin as simulated by the Canadian regional climate model (CRCM). *Journal of Hydrometeorology*, *8*(5), 969–988. doi:10.1175/JHM627.1

Nalcor Energy. (2009). *Project planning and description. Vol. 1 Part A of lower Churchill hydroelectric generation project environmental impact statement*. St. John's, NL: Nalcor Energy.

Pal, J. S., Giorgi, F., Bi, X., Elguindi, N., Solmon, F., Rauscher, S. A., … Steiner, A. L. (2007). Regional climate modeling for the developing world: The ICTP RegCM3 and RegCNET. *Bulletin of the American Meteorological Society*, *88*(9), 1395–1409. doi:10.1175/BAMS-88-9-1395

Pal, J. S., Small, E. E., & Eltahir, E. A. (2000). Simulation of regional-scale water and energy budgets: Representation of subgrid cloud and precipitation processes within RegCM. *Journal of Geophysical Research: Atmospheres (1984–2012)*, *105*(D24), 29579–29594. doi:10.1029/2000JD900415

Peixoto, J. P., & Oort, A. H. (1992). *Physics of climate*. New York, NY: Springer-Verlag.

Pope, V. D., Gallani, M. L., Rowntree, P. R., & Stratton, R. A. (2000). The impact of new physical parametrizations in the Hadley centre climate model: HadAM3. *Climate Dynamics*, *16*(2–3), 123–146. doi:10.1007/s003820050009

Rasmusson, E. M. (1968). Atmospheric water vapor transport and the water balance of North America: II. *Large-scale water balance investigations. Monthly Weather Review*, *96*(10), 720–734. doi:10.1175/1520-0493(1968)096<0720:AWVTAT>2.0.CO;2

Reichle, R. H., Koster, R. D., Dong, J., & Berg, A. A. (2004). Global soil moisture from satellite observations, land surface models, and ground data: Implications for data assimilation. *Journal of Hydrometeorology*, *5*(3), 430–442. doi:10.1175/1525-7541(2004)005<0430:GSMFSO>

Roads, J. O., Chen, S. C., Kanamitsu, M., & Juang, H. (1998). Vertical structure of humidity and temperature budget residuals over the Mississippi River basin. *Journal of Geophysical Research: Atmospheres (1984–2012)*, *103*(D4), 3741–3759. doi:10.1029/97JD02759

Roberts, J., & Snelgrove, K. (2015). Uncertainty in regional climate model mean runoff projections under climate change: Case study of Labrador's Churchill River Basin. *Atmosphere-Ocean*, in press.

Rogers, R. R., & Yau, M. K. (1984). *A short course in cloud physics* (3rd ed.). Oxford, UK: Butterworth-Heinemann.

Ruane, A. C. (2010). NARR's atmospheric water cycle components. Part I: 20-year mean and annual interactions. *Journal of Hydrometeorology*, *11*(6), 1205–1219. doi:10.1175/2010JHM1193.1

Schär, C., Lüthi, D., Beyerle, U., & Heise, E. (1999). The soil–precipitation feedback: A process study with a regional climate model. *Journal of Climate*, *12*, 722–741. doi:0.1175/1520-0442(1999)012<0722:TSPFAP>

Scinocca, J. F., & McFarlane, N. A. (2004). The variability of modeled tropical precipitation. *Journal of the Atmospheric Sciences*, *61*(16), 1993–2015. doi:10.1175/1520-0469(2004)061<1993:TVOMTP>

Seneviratne, S. I., Viterbo, P., Lüthi, D., & Schär, C. (2004). Inferring changes in terrestrial water storage using ERA-40 reanalysis data: The Mississippi River basin. *Journal of Climate*, *17*(11), 2039–2057. doi:10.1175/1520-0442(2004)017<2039:ICITWS>2.0.CO;2

Serreze, M. C., Bromwich, D. H., Clark, M. P., Etringer, A. J., Zhang, T., & Lammers, R. (2002). Large-scale hydro-climatology of the terrestrial Arctic drainage system. *Journal of Geophysical Research: Atmospheres (1984–2012)*, *107*(D2), ALT 1-1–ALT1-28. doi:10.1029/2001JD000919

Shukla, J., & Mintz, Y. (1982). Influence of land-surface evapotranspiration on the earth's climate. *Science*, *215*(4539), 1498–1501. doi:10.1126/science.215.4539.1498

Skamarock, W. C., Klemp, J. B., Dudhia, J., Gill, D. O., Barker, D. M., Wang, W., & Powers, J. G. (2005). *A description of the advanced research WRF version 2* (No. NCAR/TN-468+ STR). National Center for Atmospheric Research Boulder Colorado Mesoscale and Microscale Meteorology Div. Boulder, CO: NCAR.

Strong, G. S., Proctor, B., Wang, M., Soulis, E. D., Smith, C. D., Seglenieks, F., & Snelgrove, K. (2002). Closing the Mackenzie Basin water budget, water years 1994/95 to 1996/97. *Atmosphere-Ocean*, *40*(2), 113–124. doi:10.3137/ao.400203

Trenberth, K. E. (1991). Climate diagnostics from global analyses: Conservation of mass in ECMWF analyses. *Journal of Climate*, *4*(7), 707–722. doi:10.1175/1520-0442(1991)004<0707:CDFGAC>

Trenberth, K. E. (1998). Atmospheric moisture residence times and cycling: Implications for rainfall rates and climate change. *Climatic Change*, *39*(4), 667–694. doi:10.1023/A:1005319109110

Trenberth, K. E., Dai, A., Rasmussen, R. M., & Parsons, D. B. (2003). The changing character of precipitation. *Bulletin of the American Meteorological Society*, *84*(9), 1205–1217. doi:10.1175/BAMS-84-9-1205

Trenberth, K. E., Fasullo, J. T., & Kiehl, J. (2009). Earth's global energy budget. *Bulletin of the American Meteorological Society*, *90*(3), 311–323. doi:10.1175/2008BAMS2634.1

Verseghy, D. L. (2009). CLASS–The Canadian land surface scheme (Version 3.4), Technical documentation (Version 1.1). *Climate Research Division, Science and Technology Branch, Environment Canada*. Toronto, ON: Environment Canada.

Wang, K., & Dickinson, R. E. (2012). A review of global terrestrial evapotranspiration: Observation, modeling, climatology, and climatic variability. *Reviews of Geophysics*, *50*(2), 1–54. doi:10.1029/2011RG000373

Wang, M., & Paegle, J. (1996). Impact of analysis uncertainty upon regional atmospheric moisture flux. *Journal of Geophysical Research: Atmospheres (1984–2012)*, *101*(D3), 7291–7303. doi:10.1029/95JD02896

Water Survey of Canada. (2010). *Historical hydrometric data* [Data]. Retrieved from http://www.wsc.ec.gc.ca/applications/H2O/report-eng.cfm?yearb=&yeare=&station=03OE001&report=monthly&year=1971